Corrosion Science 51 (2009) 1299–1307

Contents lists available at ScienceDirect

Corrosion Science

journal homepage: www.elsevier.com/locate/corsci

Determination of diffusion coefficient of chloride in concrete using Warburg diffusion coefficient

R. Vedalakshmi [a,*], V. Saraswathy [a], Ha-Won Song [b], N. Palaniswamy [a]

[a] Corrosion Protection Division, Central Electrochemical Research Institute, Alagappapuram, Karaikudi, Tamil Nadu 630 006, India
[b] School of Civil Engineering, Yonsei University, Seoul 120-749, Republic of Korea

ARTICLE INFO

Article history:
Received 20 June 2008
Accepted 11 March 2009
Available online 21 March 2009

Keywords:
A. Concrete
A. Mild steel
A. Steel reinforced concrete
B. EIS
Mass loss

ABSTRACT

Assessment of diffusion coefficient of chloride (D) using chloride profile method based on Fick's law (D_{FL}) is either overestimates or underestimates the time to initiation of corrosion (T_i). An alternate method for predicting 'D' using Warburg diffusion coefficient (D_{WI}) which is determined from Electrochemical Impedance Spectroscopy technique (EIS) is established. The results reveal that EIS being non-destructive appears a promising technique to arrive at time-dependent characteristics of D_{WI} *in situ* in concrete structures. D_{WI} is an intrinsic effective diffusivity measures the diffusion of free chloride through the pore solution present in the interconnected pores. Pore constriction by pozzolanic reaction and higher chloride binding capacity reduces the D_{WI} in PPC and PSC concrete by a factor of 1.65 and 4 times that of OPC concrete in 20 MPa concrete; 1.83 and 2.52 in 30 MPa concrete; 24 and 16 times in 40 MPa concrete respectively.

1. Introduction

For estimation of durability of structures, it is highly desirable to quantify the chloride diffusion process in concrete. According to the conceptual model developed by Tutti [1] there are two distinct periods of deterioration caused by corrosion. They are initiation and propagation periods. The initiation period (T_i) is the time taken for Cl^- or CO_2 to diffuse to the steel–concrete interface and activate the corrosion. The time to initiation of corrosion is normally calculated from the diffusion coefficient of chloride (D_{eff}) using Fick's second law as follows [2]:

$$T_i = \frac{x^2}{4D_{eff}\ \mathrm{erf}^{-1}\left(1-\frac{C_x}{C_s}\right)^2} \quad (1)$$

where T_i – time for chloride to reach C_x (x,t) at cover depth x, s; x – cover of concrete, m; D_{eff} – diffusion coefficient of chloride, $m^2\ s^{-1}$; C_s – surface chloride concentration, % by weight of cement; C_x – threshold chloride concentration at which corrosion initiates on the rebar, % by weight of cement.

The governing parameters of diffusion based corrosion initiation time using Eq. (1), are concrete cover depth, chloride diffusion coefficient in concrete, surface chloride concentration and chloride threshold level. When only natural diffusion is involved different conditions/methods lead to different diffusion coefficients. After concrete has hardened, the diffusion of chloride ions is predominantly controlled by the composition and microstructure of the concrete. Diffusion of chloride is a time-dependent process. It will decrease with time since the capillary pore system will be altered as hydration products continue to form. In addition to this, some chloride ions will become chemically or physically bound as they penetrate through the pore system and form complex salts (Friedel's salt). As such it is difficult to precisely predict the diffusion coefficient. It is reported that the short term migration tests give much higher D values [3]. The most common method widely used is the measuring of chloride profile after a predetermined time and fitting this profile in Fick's second law of diffusion. Determination of concentration of chloride at known depth (C_x) by volumetric method is laborious and destructive in nature. The 'D' predicted by the migration test is a stationary value and includes only the ionic transport. 'D' predicted from natural diffusion test is a non-stationary value and take into account binding of chlorides with cement phases [4]. From the earlier studies [5] it is understood that assumption of one dimensional flow solution from the surface into a half space, a considerable scatter in chloride threshold value of rebar found in the literature and the change in surface chloride concentration with time are some of the factors that contribute to errors in the prediction of 'D' based on Fick's law. Hence the uncertainties exist in the determination of 'D' leading to a considerable error in the determination of time to initiation of corrosion. Variations of $D \pm 50\%$, could lead to variations in T_i ranging from −33% to +100% [5]. Nowadays the service life modeling is becoming a common tool for performance-based specification, an

* Corresponding author. Tel.: +04565 227550; fax: +04565 227779/227713.
E-mail address: corrveda@yahoo.co.in (R. Vedalakshmi).

0010-938X/$ - see front matter © 2009 Elsevier Ltd. All rights reserved.
doi:10.1016/j.corsci.2009.03.017

alternate approach to predict the time to initiation of corrosion is an essential one. No standard test method is established so far [6]. An accurate prediction is critical for the selection of a durable and cost effective design and for the optimization of the inspection and maintenance of built structures.

Electrical resistance measurement from Electrochemical Impedance Spectroscopy technique (EIS) represents an additional and fast developing technique in the study of cement-based materials both at micro and macro scale [7–11]. Since the flow of electrical current through hydrating paste is electrolytic, that is mainly due to the flow of ions through the pore spaces, its resistivity is an indirect measurement of porosity and diffusivity [12]. EIS is a powerful tool used in studying stationary as well as transient processes in system over conventional direct current methods. By measuring the frequency response of the impedance (resistance), much information about the reaction mechanism and mass transfer can be obtained. Lu [13] found that resistivity from impedance was an equivalent indication of the relative permeability of cement-based systems. Diaz et al. [14] established the relation between diffusion coefficient, resistance from EIS and ionic mobility.

The objective of the present investigation is to evolve a suitable methodology for the instantaneous measurement of '*D*' in actual concrete structures using EIS technique. The '*D*' determined using Warburg diffusion coefficient (D_{WI}) from the Nyquist plot is compared with the '*D*' determined from C_x using Fick's law (D_{FL}). The reliability of T_i predicted by D_{WI} will be compared with the actual rebar mass loss measurement.

2. Theoretical background

In EIS technique, the reaction kinetics and diffusion are characterized by Faradaic impedance, which is composed of the charge transfer resistance in series with the Warburg impedance (WI) describing the diffusion behaviour. Diffusion can create an impedance called a Warburg impedance. The impedance depends upon the frequency of the potential perturbation. At high frequencies, the Warburg impedance is small since diffusing reactants don't have to move very far. At low frequencies the reactants have to diffuse further, increasing the Warburg impedance.

The equation for the Warburg impedance is:

$$Z_w = \sigma_w(\omega)^{-1/2}\ (1-j) \tag{2}$$

On a Nyquist plot, the Warburg impedance appears as a diagonal line with a slope of 45°. In Eq. (2), σ_w is the Warburg coefficient, which can be defined as [15]:

$$\sigma_w = \frac{RT}{n^2F^2A\sqrt{2}}\left(\frac{1}{C_0\sqrt{D_0}}+\frac{1}{C_R\sqrt{D_R}}\right) \tag{3}$$

in which, ω – radial frequency; D_0 – diffusion coefficient of the oxidant; D_R – diffusion coefficient of the reductant; A – surface area of the electrode; n – number of electrons involved; σ_w – Warburg coefficient; C_0 – concentration of the oxidant; C_R – concentration of the reductant; F – Faraday constant; R – gas constant; T – temperature.

This form of the Warburg impedance is only valid if the diffusion layer has an infinite thickness. In the reversible reaction, which is controlled by the diffusion of chloride ions alone and diffuse under a concentration gradient, then the above equation can be reduced to

$$\sigma_w = \frac{RT}{\sqrt{2}AF^2D^{1/2}C} \tag{4}$$

For a reversible reaction of $R_{ct} \to 0$, the Randles plot either Z'' versus $\omega^{-1/2}$ or Z' versus $\omega^{-1/2}$ must intersect the origin and this can be taken as the criterion for the reversibility of the reaction.

From Eq. (4), D_{WI} can be calculated as:

$$D_{WI} = \left[\frac{RT}{\sqrt{2}AF^2\sigma_wC}\right]^2 \tag{5}$$

where D_{WI} – diffusion coefficient of chloride, $m^2\ s^{-1}$ using σ_w; A – area of electrode, m^2: σ_w – Warburg coefficient, $\Omega\ m^2\ s^{-1/2}$; C – concentration of chloride in mol m^{-3}; R – gas constant, $J\ K^{-1}\ mol^{-1}$; T – temperature, K; F – Faraday constant, $C\ mol^{-1}$.

With time when the rebar reaches the diffusion behaviour, D_{WI} was calculated using Eq. (5).

3. Experimental

3.1. Materials and mix proportions

Three mix proportions having a design compressive strength of 20, 30 and 40 MPa concrete at 28 days were used for casting the concrete specimens. The details of mix proportions are given in Table 1. Three cements namely ordinary Portland cement conforming to IS 8112 [16] equivalent to ASTM Type I cement, Portland pozzolana cement conforming to IS 1489 (Part-1) [17] and Portland slag cement conforming to IS 455 [18] were used. Chemical composition of cements used is presented in Table 2. Well graded river sand and good quality crushed blue granite were used as fine and coarse aggregates respectively. The different size fractions of coarse aggregate (20 mm down graded and 12.5 mm down graded) were taken and recombined to a specified grading. Sixteen millimeter of diameter cold twisted high yield strength deformed bar (Fe 415 grade) conforming to IS 1786 [19] was used and its chemical composition is C, 0.17%; Mn, 0.66%; Si, 0.115%; S, 0.017%; P, 0.031% and Fe, balance. Potable water was used for casting the concrete specimens.

3.2. Specimen preparation

0.15 × 0.15 × 0.15 m size concrete cubes as shown in Fig. 1 were cast. 0.1 m long CTD (cold twisted deformed) rods of 16 mm diameter were taken and pickled in inhibited hydrochloric acid solution to remove the initial rust product. In each specimen, three rods of similar dimension were embedded at 25 mm cover from one side of the specimen. For electrochemical measurement, copper wire was brazed at one end of a particular rod and that was sealed. Impedance measurement was carried out over an exposed length of 8 cm and the remaining area was sealed using epoxy compound. For determining the corrosion rate from weight-loss measurement, another two rods were embedded near to the previous one as shown in Fig. 1. Before embedding, the initial weight of the rods was recorded. While casting, all the three rebars were embedded vertically with a 25 mm cover from the top and bottom.

Table 1
Details of concrete mix proportion.

Grade	Type of cement	*w/c* ratio	Cement ($kg\ m^{-3}$)	Fine aggregate ($kg\ m^{-3}$)	Coarse aggregate ($kg\ m^{-3}$)	Characteristic compressive strength (MPa)
20 MPa	OPC	0.67	284	770	1026	27
	PPC	0.67	284	770	1026	23
	PSC	0.67	284	770	1026	28
30 MPa	OPC	0.54	352	739	1026	37
	PPC	0.54	352	739	1026	31
	PSC	0.54	352	739	1026	39
40 MPa	OPC	0.42	452	655	1026	54
	PPC	0.42	452	655	1026	42
	PSC	0.42	452	655	1026	48

Table 2
Chemical composition and physical properties of three types of cement.

Compound	Ordinary Portland cement (wt%)	Portland Pozzolana cement (wt%)	Portland slag cement (wt%)
Silicon-di-Oxide (SiO_2)	20–21	28–32	26–30
Aluminium Oxide (Al_2O_3)	5.2–5.6	7.0–10.0	9.0–11.0
Ferric Oxide (Fe_2O_3)	4.4–4.8	4.9–6.0	2.5–3.0
Calcium oxide (CaO)	62–63	41–43	44–46
Magnesium oxide (MgO)	0.5–0.7	1.0–2.0	3.5–4.0
Sulphur-tri-Oxide (SO_3)	2.4–2.8	2.4–2.8	2.4–2.8
Loss on ignition	1.5–2.5	3.0–3.5	1.5–2.5
Bogue compound composition:			
Tricalcium Silicate (C_3S)	42–45	Not applicable	Not applicable
Dicalcium Silicate (C_2S)	20–30	-do-	-do-
Tricalcium Aluminate (C_3A)	7.0–9.0	-do-	-do-
Tetra Calcium Alumino Ferrite (C_4AF)	11–13	-do-	-do-
Physical Properties:			
Pozzalanic Material used	–	Fly ash 20 wt%	GGBS 50 wt%
28 Day Compressive Strength (MPa)	62	48	53
Fineness ($m^2\ kg^{-3}$)	295	363	385

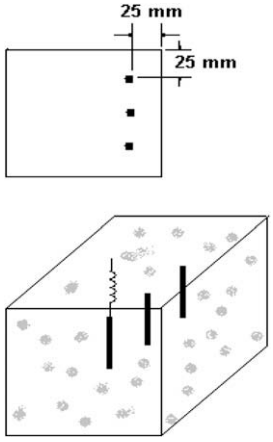

Fig. 1. Rebar arrangement in concrete specimen.

Four specimens were cast for each grade/cement. The specimens were cured at room temperature for 28 days in the potable water.

3.3. Exposure condition

After 28 days of curing, the specimens were exposed in the exposure yard. Synthetic seawater was prepared as specified in ASTM D 1141 [20]. Synthetic seawater was sprayed horizontally using spray gun once in a day for 5 days on one side of the specimen and then the specimen was air dried for the next 2 days. Thus 7 days constituted one cycle of wetting and drying and all the specimens were subjected to similar exposure condition. This test procedure simulates the atmospheric exposure of concrete structures in marine environment. The temperature, relative humidity and other parameters prevailing at the exposure site are given in Table 3. The exposure site is situated more than 2.5 km from the sea. The experiment was conducted over a period of 1765 days.

Table 3
Meteorological data.

	Maximum	Minimum
Temperature (average)	33 °C	21 °C
Relative humidity (average)	80	60
Rainfall (average)	180 mm	
SO_2	Nil	
Salinity	38 mg m^{-2} d^{-1}	

3.4. Method of measurement

Impedance measurement was made using three electrode arrangements. Stainless steel electrode of size 10×80 mm was used as an auxiliary electrode and saturated calomel electrode was used as a reference electrode. Rebar embedded in concrete acted as a working electrode. The electrode assembly was kept on a wetted sponge. The length of the counter electrode is more than the exposed length of the rebar and by means of this, current was distributed uniformly throughout the length of the rebar. Chloride solution was used as a contacting solution to reduce the contact resistance between the electrode assembly and the concrete. A small sinusoidal voltage signal of 20 mV was applied over a frequency range of 100 kHz–10 mHz using a computer controlled electrochemical analyzer (Model 6310: EC & G Instruments, Princeton applied research). Measurements were made periodically at the end 0, 80, 267, 540, 1135 and 1765 days. The impedance values were plotted on the Nyquist plot.

3.5. D_{WI} from the coefficient of Warburg impedance

The equivalent circuit of WI behaviour is given in Fig. 2a. Typical Nyquist plot with the Warburg impedance describing the diffusion-controlled reaction is shown in Fig. 2b. The analytical expression is,

$$Z = R_s + \frac{Z_F}{1 + j\omega Z_F C_{dl}} \tag{6}$$

where $Z_F = R_{ct} + WI$

From the plot it can be seen that, in the high frequency region, the experimental curve is a semi-circle and in the low frequency region, it is a straight line having a slope of -1. Correspondingly, at the high frequency limit, Warburg impedance becomes unimportant. At the low frequency limit it will approach the limiting form as shown below [21]:

$$Z' = R_s + R_{ct} + \sigma_w \omega^{-1/2} \tag{7}$$

$$Z'' = \sigma_w \omega^{-1/2} + 2\sigma_\omega^2 C_{dl}. \tag{8}$$

Elimination of ω leads to

$$Z'' = Z' - R_s + R_{ct} + 2\sigma_w^2 C_{dl} \tag{9}$$

where, σ_w is the coefficient of Warburg impedance, which can be obtained from the intersection of the straight line on the real axis as shown in Fig. 2b which is given below:

$$\sigma_w = \left[\frac{R_s + R_{ct} - x}{2C_{dl}}\right]^{1/2} \tag{10}$$

where R_s – concrete resistance, $\Omega\ m^2$; R_{ct} – charge transfer resistance, $\Omega\ m^2$; C_{dl} – capacitance of electrode–electrolyte interface $F\ m^{-2}$; σ_w – Warburg coefficient, $\Omega\ m^2\ s^{-1/2}$.

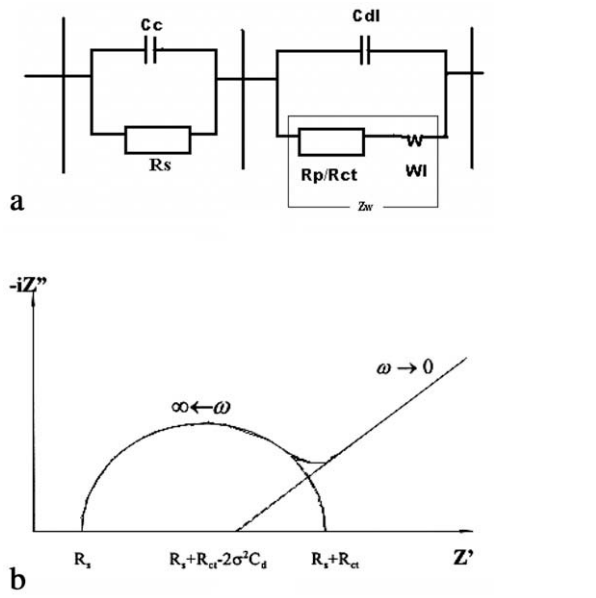

Fig. 2. Method of determining σ_w from Nyquist plot: (a) Equivalent circuit (b) Nyquist plot with Warburg impedance.

As shown in Fig. 2b, "$R_s + R_{ct}$" represent the resistance of the concrete whereas the "x" represent the resistance due to reaction kinetics at the steel interface. If "x" deducted from the "$R_s + R_{ct}$", it represents the resistance due to diffusion of free chloride through the pore solution present in the cover concrete. Substituting the value of σ_w in Eq. (5), the D_{WI} was calculated. D_{WI} is dependent of x, t and it represent the diffusion of free chloride through the pore solution present in the cover concrete.

3.6. Determination of D_{FL} using Fick's law

The water-soluble chloride content (C_x) was determined by volumetric analysis using silver nitrate method [22,23]. The concrete sample near the rebar level i.e., at 25 mm cover depth was collected after the exposure period of 775 and 1135 days. The sample was powdered and sieved through a 600 μm sieve. Then this powder was mixed with distilled water at the ratio of 1:3 by weight. This mixture was taken in a closed glass tube and shaken for 10 min and kept for 48 h to dissolve the Cl^- ions completely. After 48 h, the solution was filtered and used to determine the Cl^- ion concentration. Using potassium chromate as an indicator, 5 ml of filtered solution was titrated against 0.01 N silver nitrate solution. From the titrated value, the Cl^- ion concentration (C_x) was calculated. Using the concrete sample taken from 0 to 5 mm depth, the surface chloride concentration (C_s) was determined. After converting the concentration of C_x and C_s into a % of chloride by weight of cement, using Fick's law, the D_{FL} was calculated as below:

$$C_x = C_s\left(1 - \mathrm{erf}\left[\frac{x}{2\sqrt{D_{FL}t}}\right]\right) \quad (11)$$

The D_{FL} was calculated at the end of 775 and 1135 days and the average value was reported. D_{WI} from σ_w represents the diffusion of chloride ions through the pore solution. To compare this value, for determining D_{FL}, water-soluble chloride was determined. It is widely recognized that the corrosion of rebar is caused by water-soluble (free) chloride present in the concrete pore solution and hence in the present study both D_{WI} and D_{FL} represent the diffusion of free chlorides only.

3.7. Determination of corrosion rate from mass loss method

Periodically at the end of 775, 1135, 1528 and 1765 days, the rods were visually examined for the extent of rust. After pickling the rebars in inhibited hydrochloric acid as specified in ASTM G1 [24], the final weight was measured. From the initial and final weight, the corrosion rate in μm y^{-1} was calculated.

3.8. Determination of chloride threshold value and time to initiation of corrosion

For calculating time to initiation of corrosion (T_i) from D_{WI} and D_{FL}, using Eq. (1), the determination of threshold chloride concentration for initiation of corrosion (C_x) is an important parameter. The threshold chloride concentration is the concentration at which breakdown of passive film occurs and corrosion initiates on the rebar. In the present study, it was arrived by taking the chloride concentration at which the rebar having a mass loss of 0.006 g cm^{-2} (equivalent to 0.09% of mass loss) [25]. Periodically at the end of 775, 1135, 1528 and 1765 days of exposure, the Cl^- (as described in Section 3.6) and rebar mass loss were determined. From the plot of C_x versus rebar mass loss, the chloride value corresponding to the mass loss of 0.006 g cm^{-2} has been taken as threshold chloride concentration. After arriving the threshold chloride concentration, T_i was calculated using Eq. (1).

4. Results

4.1. D_{WI}

Fig. 3 compares the Nyquist plot of rebar in 30 MPa-PPC concrete with exposure period. Initially at the end of 80 days, the slope of the low frequency arc is −3.72 and gets decreased to −1.10 at the end of 540 days. At the end of 1765 days, the straight line gets disappeared and showed that the strong decrease of capacitive part in the impedance response shall be correlated to the diffusion phenomena of cover concrete. Concrete specimens, exposed to chloride solution of a certain concentration for a sufficient period of time, then all the pores in the micro structure are filled with the chloride solution and capillary paths are established for diffusion. Under salt-spray test, in the cover concrete, the chloride ion concentration (30 g L^{-1}) is higher when compared to other ions, it has been assumed as diffusion behaviour observed in the Nyquist

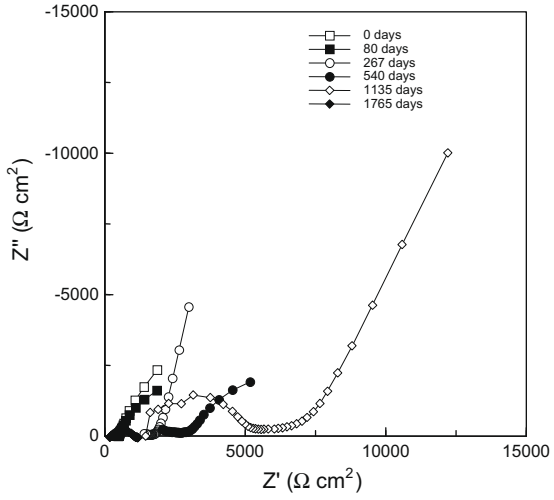

Fig. 3. Nyquist plot of rebar embedded in M30-PPC concrete versus exposure period.

plot is only due to chloride ions. From the curve, it can be also seen that in the high frequency region, the experimental curve is a semicircle and in the low frequency region, it is a straight line. When the low frequency arc of impedance behaviour reaches to −1 (with a slope equal to 45°), ensures the chloride concentration gradient is established in the cover concrete and that impedance was termed as 'Warburg impedance' and used for the determination of σ_w. From Fig. 3, it is clearly evident that in 30 MPa-PPC concrete, initially at the end of 80 days as the availability of chloride ions in the cover concrete is very negligible and due to the presence of large and non-ideal apparent interfacial capacitance at the steel/concrete interface the slope is −3.72. After exposure to chloride environment for a period of 540 days, the diffusion of chloride ions decreases the slope from the value of −3.72 to −1.1. Depends upon the porosity of the concrete, the time taken to reach the Warburg impedance (WI) is varied. Fig. 4 compares the WI behaviour of three cements in 30 MPa concrete. From the plot it can be clearly understood that for OPC it takes 80 days whereas for PPC and PSC it is 540 and 1135 days respectively. In PPC and PSC concrete, the formation of additional calcium silicate hydrates during the pozzolanic reaction fills the pores and increases the tortuosity. The discontinuity through interconnected pores reduces the rate of diffusion of chloride and due to this, the time taken to reach WI behaviour in PPC and PSC concrete is increased.

Fig. 5 compares the Randles plot of rebar embedded in 30 MPa concrete. For a reversible reaction, $R_{ct} \rightarrow 0$, the Randles plot ($\omega^{-1/2}$ versus Z″) intersect the origin, the criterion for the reversibility of the reaction is satisfied. The reaction is mainly controlled by diffusion of chloride ions alone since diffusion is a transfer of mass by random motion of free chlorides ions in the pore solution resulting in a net flow from regions of higher (top surface) to regions of lower concentration (near rebar). The concrete specimens under this condition can be considered to be an electrochemical system and hence the rate of diffusion can be determined using σ_w. In chloride-induced corrosion, initially, the rebar is under mixed kinetic and diffusion-controlled reaction and maintains the passive condition till the chloride concentration reached its threshold level. During this period, the rate of charge transfer resistance of rebar is comparatively less. Though the film formation (Portlandite) is occurring at the steel -concrete interface as a first step, when the chloride available near the rebar surface reaches its threshold level then initiates corrosion. Hence D_{WI} denotes the diffusion process occurring through the cover concrete that affect the reaction kinetic at the steel–concrete interface just before the corrosion starts and indicated distinctly by the low frequency arc having a slope of −1 (45°).

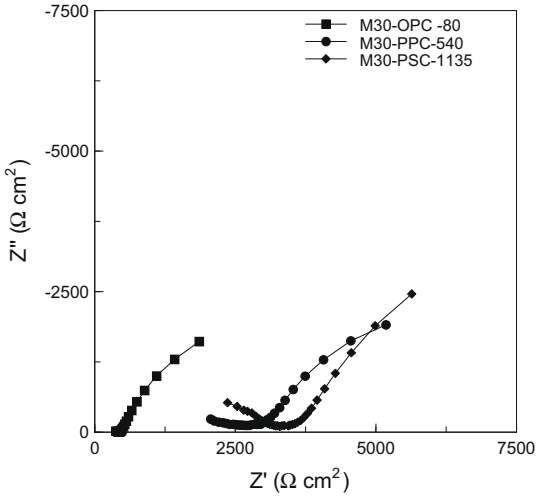

Fig. 4. Warburg impedance behaviour of OPC, PPC and PSC after an exposure period of 80, 540, 1135 days respectively in 30 MPa concrete.

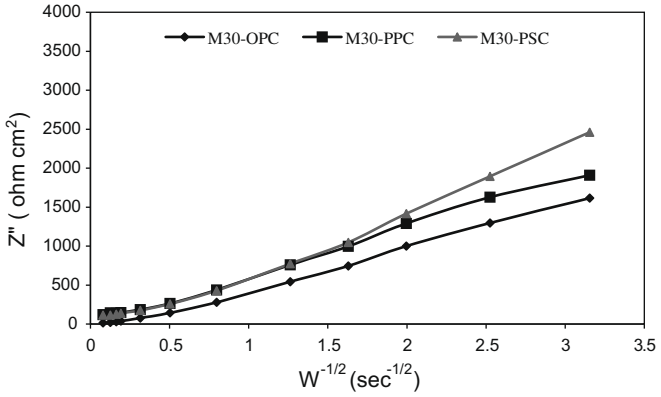

Fig. 5. Randles plot of rebar embedded in 30 MPa concrete after an exposure period of 80 days (OPC), 540 days (PPC), 1135 days (PSC).

Similar to Cl^- ion diffusion, OH^- ions also move from the inner side of the concrete to the outer surface (leaching process) when concrete exposed under immersion/splash zone condition. But in the present study, the experiment was conducted under atmospheric condition, the rate of diffusion of OH^- ions is very much less as there is no sufficient concentration gradient exists. The average OH^- ions concentration at the rebar level was also estimated from the acid-base titration and found it was 0.121 mol L^{-1} in OPC concrete and 0.036 mol L^{-1} in blended cement concretes. The values are not changed significantly upto the period of 1135 days. During this period, the concentration of chloride ions only changed with time, hence it has been assumed that the change in low frequency arc in the Nyquist plot is only due to chloride ions only. Other cations such as Na^+, K^+ and Ca^{2+} are generally less mobile than anions [26].

Fig. 6 compares the Warburg impedance behaviour of rebar in 20 and 40 MPa concrete whereas Fig. 4 compares in 30 MPa concrete respectively. From the plots, by extrapolating the low frequency arc of each cement as shown in Fig. 2b, σ_w was determined. Table 4 compares the σ_w of three cements in three concretes. Data highlights that with an increase in strength of the concrete, the σ_w also increases. From the table it can be also seen that the D_{WI} of 20 MPa-PPC concrete is 1.65 times lesser than that of OPC concrete whereas in PSC concrete it is 4 times lower than that of OPC concrete. Similarly the value is 1.83 and 2.52 times lower in 30 MPa concrete; 24 and 16 times lower in 40 MPa concrete respectively.

4.2. D_{FL}

Table 5 compares the D_{FL} at the end of 775 and 1135 days. With the time of exposure, D_{FL} is increased in 20 MPa concrete whereas it get decreased in 30 and 40 MPa concretes and confirms that the D_{FL} is time-dependent one and varies depending upon the concrete properties.

4.3. D_{WI} versus D_{FL}

Table 4 also compares the 'D's determined by both the methods. The value determined by D_{WI} is higher than that of D_{FL}. In D_{WI}, the diffusion of chloride through the pore solution is measured and the rate is mainly depending upon the size of the interconnected pore and hence it is an effective diffusivity. In the case of D_{FL}, when powdering the concrete samples, the chloride ions adsorbed into

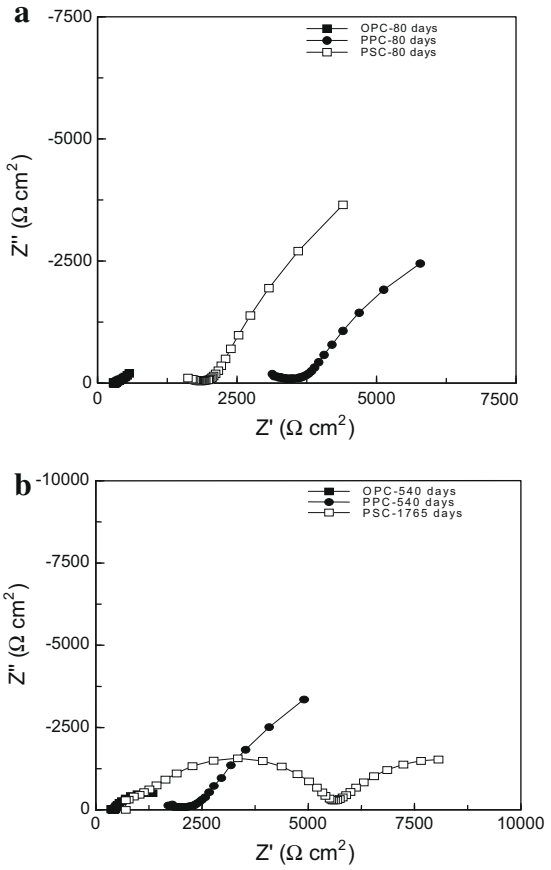

Fig. 6. WI behaviour of rebar embedded in (a) 20 MPa, (b) 40 MPa concrete.

Table 4
Comparison of D_{WI} versus D_{FL}.

Grade/type of cement	$\sigma_w \times 10^{-4}$ ($\Omega\ m^2\ s^{-1/2}$)	$D_{WI} \times 10^{-12}$ ($m^2\ s^{-1}$)	$D_{FL} \times 10^{-12}$ ($m^2\ s^{-1}$)
20 MPa-OPC	0.210	4.84	2.00
20 MPa-PPC	0.270	2.92	1.05
20 MPa-PSC	0.420	1.21	1.20
30 MPa-OPC	0.242	3.67	1.45
30 MPa-PPC	0.326	2.00	1.65
30 MPa-PSC	0.381	1.46	0.62
40 MPa-OPC	0.309	2.23	1.50
40 MPa-PPC	1.502	0.094	1.81
40 MPa-PSC	1.229	0.141	0.59

the layers of hydrated/unhydrated cement phases and aggregates are also get released in addition to free chlorides and hence it is an apparent one. In chloride transport mechanism, the diffusion of chloride occurs only through the pore solution present in the interconnected pores and D_{WI} measures this phenomenon more accurately compared to that of D_{FL}. In addition to this, in EIS technique, diffusion of chloride alone is measured in a quasi-static state, the value should be more reliable.

4.4. Determination of chloride threshold concentration (C_x)

Fig. 7 correlates the rebar mass loss with chloride content of all the three cements in 20, 30, 40 MPa concrete respectively. The correlation coefficient (R) between them varies from 0.76–0.91

Table 5
Comparison of D_{FL}.

Grade/type of cement	Water-soluble chloride (% by weight of cement) Exposure period (days)		D_{FL}, 775 × 10^{-12} ($m^2\ s^{-1}$)	D_{FL}, 1135 × 10^{-12} ($m^2\ s^{-1}$)	D_{FL}, average × 10^{-12} ($m^2\ s^{-1}$)
	775	1135			
20 MPa-OPC	3.212	4.226	2.0	2.1	2.0
20 MPa-PPC	0.676	2.536	0.9	1.2	1.05
20 MPa-PSC	0.779	2.029	1.0	1.4	1.2
30 MPa-OPC	1.781	2.397	1.6	1.3	1.45
30 MPa-PPC	1.781	3.356	1.6	1.7	1.65
30 MPa-PSC	0.137	0.411	0.60	0.64	0.62
40 MPa-OPC	1.813	1.440	1.9	1.1	1.50
40 MPa-PPC	1.173	3.20	1.4	2.22	1.81
40 MPa-PSC	0.213	0.107	0.70	0.47	0.59

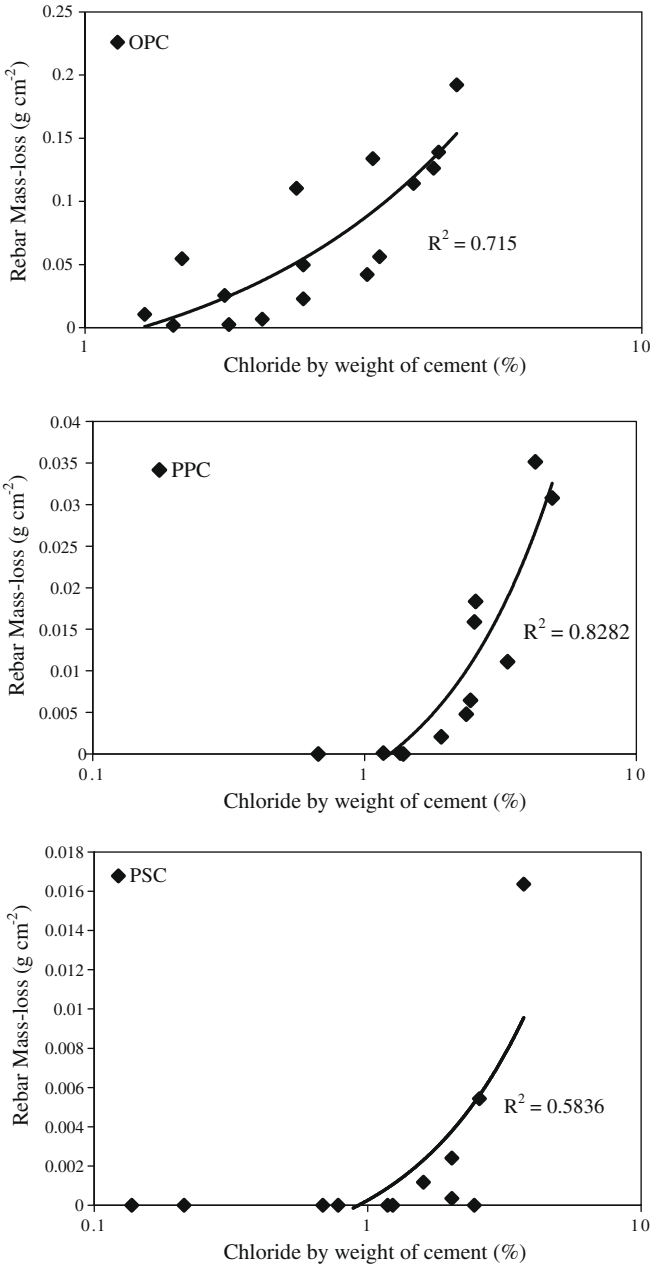

Fig. 7. Rebar mass loss versus chloride content.

Table 6
Comparison of T_i.

Grade/type of cement	T_i from D_{WI} (days)	T_i from D_{FL} (days)	Corrosion rate ($\mu m\ y^{-1}$)		
			EIS		Mass loss
			At the end of $T_i D_{WI}$	$T_i D_{FL}$	
20 MPa-OPC	309	747	5.4	17.29	25.2 (775 days)
20 MPa-PPC	658	1602	0.4	2.99	7.4 (1765 days)
20 MPa-PSC	1556	1569	1.72	1.72	0.8 (1528 days)
30 MPa-OPC	474	1199	2.80	27.49	12.40 (775 days)
30 MPa-PPC	1167	1374	1.80	2.54	5.2 (1528 days)
30 MPa-PSC	1486	3640	1.13	>9.43	0.6 (1528 days)
40 MPa-OPC	938	1394	3.17	6	0.7 (1135 days)
40 MPa-PPC	31488	1651	>0.1	0.1	0.7 (1765 days)
40 MPa-PSC	20266	5974	>1.3	>1.3	1.5 (1765 days)

indicated that the rebar mass loss increased linearly with the chloride content. It can be seen that for the negligible mass loss of $0.006\ g\ cm^{-2}$, the OPC, PPC and PSC can tolerate up to 1.813, 2.536 and 2.453% chloride by weight of cement respectively. In blended cement concrete it is 1.4 times higher than that of OPC concrete. The above experimentally arrived values were taken as the threshold chloride concentration (C_x) at the rebar level, to calculate the time to initiation of corrosion using both '*D*'s.

4.5. Time to initiation of corrosion (T_i)

Table 6 compares the T_i using D_{WI} and D_{FL}. From the table it can be seen that T_i predicted by D_{WI} is less than that of D_{FL}. The accuracy of T_i predicted by D_{WI} was ensured by comparing the value with the corrosion rate (CR) of rebar determined from EIS. For example, at the end of 267 days, the CR of rebar embedded in 20 MPa-OPC concrete is $5.4\ \mu m\ y^{-1}$ and increases to $13.2\ \mu m\ y^{-1}$ at the end of 540 days. As per the criteria proposed by the Andrade [27], if the CR is 1.2–5.8 $\mu m\ y^{-1}$, it indicates low corrosion rate and if it is more than $11.6\ \mu m\ y^{-1}$, it is high corrosion rate. When comparing the data with the above criteria, it is clearly evident that CR at the end of T_i, D_{WI} (267 days) comes under low corrosion rate whereas at the end of T_i, D_{FL} comes under high corrosion rate. T_i is the time taken by the chloride ions reached on the rebar surface and corrosion just initiated on it, at that time CR should be very negligible. It has been proved that T_i from D_{WI} is in close agreement with the CR from EIS whereas it was either overestimated or underestimated by D_{FL} as the CR is higher. This is observed repeatedly in all the three grades of OPC concrete studied. In PPC and PSC concrete, the CR at the end of T_i, D_{WI} is $<1.2\ \mu m\ y^{-1}$ and comes under passive condition whereas at the end of T_i, D_{FL}, the CR is between 1.2–5.8 $\mu m\ y^{-1}$ and comes under low corrosion. Conceptually T_i can be checked either destructively by mass loss measurement or non-destructively by EIS measurement. The mass loss measurement could not be done at the end of T_i, since the change in mass loss is very negligible and could not be estimated and hence CR from EIS has been compared. To have a sufficient mass loss, the specimens were allowed to corrode some more time and then CR was estimated and compared with the T_i. For example, in 20 MPa-OPC concrete, the CR from mass loss measurement at the end of 775 days is $25.2\ \mu m\ y^{-1}$ and such higher CR is possible only when the corrosion started at the end of 309 days. Similarly in 30 MPa-OPC concrete, T_i determined from D_{WI} is 474 days and CR at the end of 775 days is $12.4\ \mu m\ y^{-1}$. It is inferred that the CR estimated from mass loss measurement is in close agreement with the T_i determined from D_{WI}.

The above results also confirmed by observing the extent of rust on the rebar at the end of 1135 days as given in Fig. 8. In 20 and 30 MPa-OPC concrete (Fig. 8a and b), the rust spreads throughout the length of the rebar whereas negligible rust is observed in 40 MPa concrete (Fig. 8c) which are very well in agreement with the T_i from D_{WI}. As T_i gets delayed, the rebar embedded in PPC and PSC concretes show negligible rusting.

5. Discussion

5.1. Influence of type of test method on measured 'D'

In actual concrete structures, the rate of chloride diffusion into the concrete is decreased with time due to the hydration of cement and chloride binding. Because of change in either surface chloride concentration or time-dependent characteristics of '*D*', the D_{FL} based on Fick's law is not applicable to long term chloride

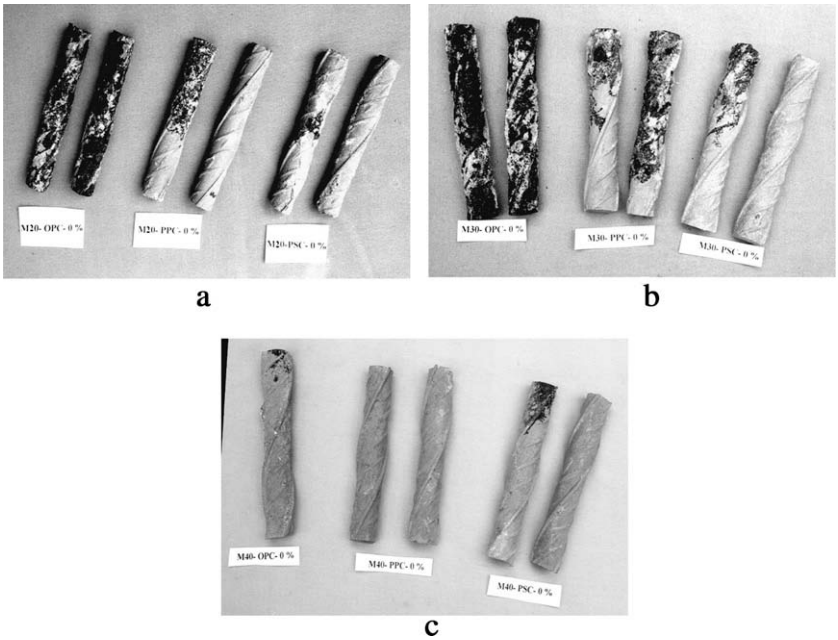

Fig. 8. Extent of rust on the rebar after 1135 days of exposure (a) 20 MPa concrete, (b) 30 MPa concrete, (c) 40 MPa concrete.

transport in concrete. It is widely accepted that the transport behaviour of chloride ions in concrete is a more complex and complicated process that can be described by Fick's law of diffusion [28] and the D_{FL} can be characterized as semi-empirical, resulting an "apparent effective diffusivity". The instantaneous measurement of '*D*' in the cover concrete of structures is an essential one for accurate prediction of T_i. It is reported [29] that the depassivation of rebar occurs in chloride-contaminated concrete by only free chlorides (water-soluble). It is important that the '*D*' determined by any method should reflect the diffusion of free chloride through the pore solution or otherwise it may be either conservative or unconservative estimate of service life. From Table 6, it can be seen that, T_i is overestimated by D_{FL}. As the drawbacks present in the conventional method has been overcome by D_{WI}, T_i by D_{WI} is more reliable which is proven by determining the CR from EIS and subsequently by mass loss measurement.

The proposed electrode arrangement is normally used for measuring the corrosion rate of rebar embedded in concrete specimens under laboratory condition in which the rebar area is known. In actual concrete structures where the rebar area is unknown, to confine the electrical signal to the known rebar area, the guard ring assembly shall be used. The advantage of proposed methodology is there is no separate sensor assembly is required for monitoring the transport properties of chlorides through the cover concrete as reported in earlier investigations [30,31]. Shi et al [21] fixed the two stainless steel plates on both the sides of the concrete specimens and found σ_w from the slope of the Randles plot.

In the present study, the rebar embedded inside the concrete was used as one electrode whereas stainless steel electrode fixed on the surface was used as another electrode and the diffusion of chloride through the cover concrete between the two electrodes was measured. The advantage of the proposed method is '*D*' can be measured at any time at site non- destructively. The measured '*D*' is inclusive of environmental parameters such as age of concrete, temperature, relative humidity and chloride convection by moisture transport when the concrete is under wet condition. The advantages of EIS technique over other DC technique are (i) the applied AC amplitude is only 20 mV and hence the disturbance of electrode surface is less (ii) measurement is easy and accurate (iii) the time-dependent characteristics of '*D*' can be determined *in situ* instantaneously.

In chloride-induced corrosion, the initiation and propagation of corrosion is mainly depends upon the concentration of chlorides and oxygen. The concentration of Cl^- ions, CO_2 and permeability of concrete are the main influencing parameters during the initiation period [1]. During the propagation period, the rate of corrosion is limited by the availability of oxygen at the steel surface and it depends on concrete quality, cover, temperature and relative humidity. The prediction of '*D*' plays a major role during the initiation period and once corrosion is initiated on the rebar surface, the time to cracking (T_p) mainly depends upon the cover of concrete, diameter of the rebar and mechanical properties of the concrete [32].

5.2. Influence of type of cement on measured 'D'

D_{WI} of PPC and PSC concrete is less than that of OPC concrete and the trend is not changed if the strength of the concrete is changed. In blended cements, the chloride binding capacity is higher and this is due to: (i) higher calcium–silicate–hydrate (C–S–H) content trap more amount of chloride ions and reduces the availability of free chloride ions (ii) the pore restructuring by pozzolanic reaction products may decrease the intrinsic diffusivity (iii) the Al_2O_3 content in PPC and PSC cement is 10–12% whereas in OPC is 5%, an additional alumina react with chloride and forms chloroaluminate leading to a reduction of free chlorides [33] (iv) the alumina fraction of glass phase allowed the dissolution of Al^{3+} ions into an alkaline pore solution and pozzolanic reaction consumes the released hydroxyl ions. To maintain the ionic neutrality, more number of chloride ions was adsorbed into the interlayers of CSH [34]. These factors contributed to the reduction of free chloride ions availability, which decreased the D_{WI}. Compared to OPC concrete, D_{WI} was found to be decrease in PPC and PSC concrete by a factor of 1.65 and 4 times that of OPC concrete in 20 MPa concrete; 1.83 and 2.52 in 30 MPa concrete; 24 and 16 times in 40 MPa concrete respectively.

5.3. Threshold chloride concentration

When looking earlier investigations [35–37] it is observed that the chloride ions concentration at which corrosion initiated was determined when (i) the potential of rebar reaches to −270 mV versus SCE (Saturated Calomel Electrode) (ii) the I_{corr} of rebar embedded in concrete reached to 0.35–1 μA cm^{-2} (iii) the R_p value of the rebar starts to get decreased (iv) using the values specified by ACI 210, ACI 222 and BIS 8110. When analyzing the results obtained by other investigators, it is observed that the threshold concentration reported in most of the cases is on cement mortar using electrochemical technique. These values may be different for concrete mixes made with different cement composition and *w*/*c* ratio and for concrete mixes incorporating mineral admixtures. The values specified in specification are only codal limits and not true threshold values for onset of corrosion. Because of above foresaid reasons, it is more appropriate to use experimentally arrived values than the value reported by other investigators. Haque and Kayyali reported [29] that 1.15% chloride (water-soluble) by weight of cement as threshold chloride concentration in medium strength concrete. In the present study 0.006 g cm^{-2} of mass loss has been taken as the limit for assessing the threshold chloride concentration and due to this, the value obtained (1.813) is slightly higher than the value reported in earlier investigations.

6. Conclusions

1. When concrete specimens subjected to chloride environment, the rebar embedded in them attains mixed kinetic and diffusion-controlled reaction, coefficient of Warburg impedance (σ_w) in the Nyquist plot able to predict the diffusion coefficient of chloride (D_{WI}) more precisely than the conventional method (D_{FL}).
2. Randles plot ($\omega^{-1/2}$ versus Z″) of Warburg impedance behaviour intersect the origin satisfy the criterion for the reversibility of reaction.
3. D_{WI} reflects the time-dependent characteristics of '*D*' more accurately and measures only diffusion of chloride through the pore solution present in the interconnected pores. Both pore size and tortuosity factors are incorporated when measuring the D_{WI}, it is an intrinsic effective diffusivity. D_{WI} is capable of measuring '*D*' at site in a non-destructive way.
4. Time to initiation of corrosion is delayed considerably in PPC and PSC concretes compared to that of OPC concrete. Added mineral admixtures such as fly ash, slag along with cement and reduced *w*/*c* ratio constricts the pore size and increased the tortuosity leads to reduction of D_{WI} and delays the T_i.

Acknowledgements

The authors thank the Director, CECRI, Karaikudi for his kind permission to publish this article. The authors also gratefully acknowledge the support from Center for Concrete Corea, South Korea for financial assistance.

References

[1] K. Tutti, Corrosion of steel in concrete. Report 4-82, Swedish Cement and Concrete Research Institute, Sweden, 1982.
[2] Y. Liu, A.R. Weyer, Modeling the time to corrosion cracking in chloride contaminated reinforced concrete structures, ACI Mater. J. 95 (1998) 675–681.
[3] D.J. Cook, I. Hinczak, M. Jedy, H.T. Cao, Migration tests on concrete, Proceedings of 3rd International conference on fly ash, silica fume, slag and natural pozzolana in concrete, ACI SP-114 (1989) 1467–1483.
[4] J. Zhang, Z. Lounis, Sensitivity analysis of simplified diffusion based corrosion initiation time model of concrete structures exposed to chlorides, Cement Concrete Res. 36 (2006) 1312–1323.
[5] M. Nokken, A. Boddy, R.D. Hooton, M.D.A. Thomas, Time-dependent diffusion in concrete-three laboratory studies, Cement Concrete Res. 36 (2006) 200–207.
[6] C. Andrade, M. Castellote, A.AlonsoG. Gonzalez, Non-steady state chloride diffusion coefficients obtained from migration and natural diffusion tests. Part 1. Comparison between several methods of calculation, Mater. Struct. 33 (2000) 21–28.
[7] M. Cabeza, P. Merino, A. Mirind, X.R. Nova, I. Sanchez, Impedance spectroscopy study of hardened Portland cement pastes, Cement Concrete Res. 32 (2002) 881–891.
[8] W.J. McCarter, R. Brousseau, The A.C. response of hardened cement paste, Cement Concrete Res. 20 (1990) 891–900.
[9] Ping Gu, Ping Xie, J.J. Beaudoin, R. Brousseau, A.C. impedance spectroscopy (I) : A new equivalent circuit model for hydrated Portland cement paste, Cement Concrete Res. 22 (1992) 833–840.
[10] P. Xie, P. Gu, Z. Xu, J.J. Beaudoin, A rationalized a.c. impedance model for micro structural characterization of hydrating cement systems, Cement Concrete Res. 23 (1993) 359–367.
[11] V.S. Ramachandran, J.J. Beaudoin, Study of early hydration of high alumina cement containing phosphoric acid by impedance spectroscopy, J. Mater. Sci. Lett. 14 (1995) 503–505.
[12] Z. Liu, J.J. Beaudoin, An assessment of the relative permeability of cement systems using AC impedance techniques, Cement Concrete Res. 29 (1999) 1085–1090.
[13] X. Lu, Application of the Nernst-Einstein equation to concrete, Cement Concrete Res. 27 (1997) 293–302.
[14] B. Diaz, X.R. Novoa, M.C. Perez, Study of the chloride diffusion in mortar: A new method of determining diffusion coefficients based on impedance measurements, Cement Concrete Comp. 28 (2006) 237–245.
[15] A.J. Bard, L.R. Faukner, Electrochemical Methods, John Wiley & Sons, New York, 1980.
[16] IS 8112, Specification for 43 grade ordinary Portland cement, BIS Standards, New Delhi, 1989.
[17] IS 1489 (Part 1), Specification for Portland pozzolana cement (fly ash based), BIS standards, New Delhi, 1991.
[18] IS 455, Specification for Portland slag cement, BIS Standards, New Delhi, 1989.
[19] IS 1786, Specification for high strength deformed steel bars and wires for concrete reinforcement, BIS Standards, New Delhi, 1985.
[20] ASTM D1141-98, Standard Practice for the preparation of substitute Ocean water, ASTM Standards, vol. 11.02, pp.28–30.
[21] M. Shi, Z. Chen, J. Sun, Determination of chloride diffusivity in concrete by AC impedance technique, Cement Concrete Res. 29 (1999) 1111–1115.
[22] P.S. Mangat, B.T. Molloy, Influence of PFA, slag and micro-silica on chloride induced corrosion of reinforcement in concrete, Cement Concrete Res. 21 (1991) 819–834.
[23] S. Muralidharan, R. Vedalakshmi, V. Saraswathy, N. Palaniswamy, Studies on the aspects of chloride ion determination in different types of concrete under macro cell corrosion condition, Build. Environ. 40 (2005) 1275–1281.
[24] ASTM G1-03, Standard practice for preparing, cleaning and evaluating corrosion test specimens, ASTM Standards, vol. 03.02, pp. 9–14.
[25] M. Thomas, Chloride thresholds in marine concrete, Cement Concrete Res. 26 (1996) 513–519.
[26] P.W. Atkins, Physical Chemistry, fifth ed., Oxford University Press, Oxford, UK, 1994.
[27] C. Andrade, C. Alonso, J. Gonzalez, An initial effort to use the corrosion rate measurements to estimating the rebar durability, in: V.S. Berke, V. Chaker, D. Whiting (Eds.), Corrosion Rates of Steel in Concrete. ASTM – STP 1065, American Society for Testing and Materials, Philadelphia, 1990, pp. 29–37.
[28] V.G. Papadakis, Effect of supplementary cementing materials on concrete resistance against carbonation and chloride ingress, Cement Concrete Res. 30 (2000) 291–299.
[29] M.N. Haque, O.A. Kayyali, Aspects of chloride ion determination in concrete, ACI Mater. J. 92 (1995) 532–541.
[30] W.J. McCarter, T.M. Chrisp, G. Starrs, P.A.M. Basheer, J. Blewett, Field monitoring of electrical conductivity of cover-zone concrete, Cement Concrete Comp. 27 (2005) 809–817.
[31] W.J. McCarter, T.M. Chrisp, A. Butler, P.A.M. Basheer, Near surface sensors for condition monitoring of cover-zone concrete, Constr. Build. Mater. 15 (2001) 115–124.
[32] T.EI. Maaddawy, K. Soudki, A model for prediction of time from corrosion initiation to corrosion cracking, Cement Concrete Comp. 29 (2007) 168–175.
[33] S. Li, D.M. Roy, Investigations of relation between porosity, pore structure and Cl^- diffusion of fly ash and blended cement pastes, Cement Concrete Res. 16 (1986) 749–759.
[34] A.K. Suryavanshi, J.D. Scantlebury, S.B. Lyon, Mechanism of Friedal's salt formation in cements rich in tri-calcium aluminate, Cement Concrete Res. 26 (1996) 717–727.
[35] S.E. Hussain, A.L. Gahtani, Rasheeduzzafar, Chloride threshold for corrosion of reinforcement in concrete, ACI Mater. J. 94 (1996) 534–538.
[36] C. Alonso, C. Andrade, M. Castellote, P. Castro, Chloride threshold values to depassivate reinforcing bars embedded in a standardized OPC mortar, Cement Concrete Res. 30 (2000) 1047–1055.
[37] R.P. Khatri, V. Srivivatnanon, P. Heeley, Critical polarization resistance in service life determination, Cement Concrete Res. 34 (2004) 829–837.